

# **Optical trapping of director structures and defects in liquid crystals using laser tweezers**

**Ivan I. Smalyukh<sup>1,2\*</sup>, Daniel S. Kaputa<sup>1</sup>, Aliaksandr V. Kachynski<sup>1</sup>, Andrey N. Kuzmin<sup>1</sup>,  
and Paras N. Prasad<sup>1</sup>**

*1*





was steered in the horizontal plane by a computer-controlled galvano-mirror pair and visualized by a co-localized low-power ( $<100\mu W$ ) beam of a HeNe laser ( $633nm$ ). The vertical position of the laser trap was controlled by a piezo-stage with  $0.1\mu m$  accuracy. Simultaneously with optical trapping, we conducted polarizing microscopy (PM) and bright-field optical microscopy observations using a charge-coupled device (CCD) camera

domain, and twists by  $180^\circ$  as one moves to the domain's perimeter in all radial directions. This  $\pi$ -twist of the director matches overall untwisted homeotropic ( $\hat{N}$  perpendicular to the cell substrates) director field in the rest of the LC cell.

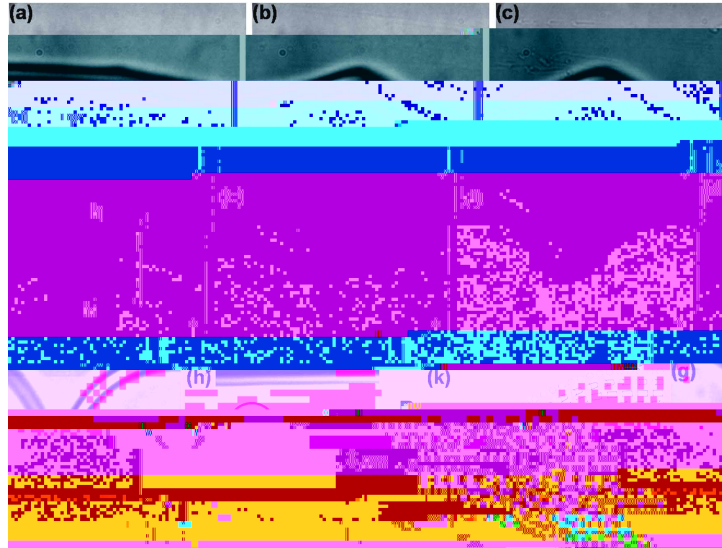


Fig. 3. Stretching of an optically trapped dislocation in a lamellar LC by moving the sample using a stage: (a, 1.1 MB) video sequence and (b-g) extracted representative image frames. The directions of the sample displacement are shown by the black arrows in (a-g). (h) Layers profile in the vertical FCPM cross-section that was obtained (before the optical trapping experiments) in the plane orthogonal to the dislocation, as shown by the h-h line in (d). Schematics of the director field around the defect core shown by the red circle in (h). Linear polarization direction of the trapping laser beam is along the y-axis in (a-g). FCPM polarization direction in (h) is along the defect line. Polarizing microscopy textures (a-g) were obtained with the crossed polarizer and analyzer along the vertical/horizontal image edges.

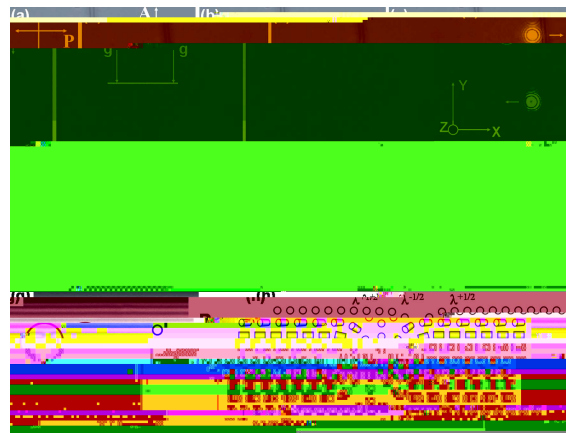


Fig. 4. Laser manipulation of a disclination quadrupole: (a, 1.9 MB) video sequence and (b-f) extracted frames. A single beam is time-shared between the two IR traps visualized in (a) by a HeNe laser beam co-localized with the trapping beam. The traps are slowly shifted as shown by white arrows in (a) and the disclinations are stretched (a-f) until they escape from the traps (f), because of their line tension. (g) Layers structure visualized by the FCPM for the vertical cross-section perpendicular to the cluster, as marked by the g-g line in (b). (h) The director field around the disclination cluster shown by the red circle in (g). Linear polarization of the laser beam used for manipulation is along the y-axis in (a-f). FCPM polarization direction is normal to the image and along the cluster in (g). Textures (a-f) were obtained with the crossed polarizer and analyzer along the image edges.

### *3.2 Laser trapping and manipulation with low-intensity beams*

Linearly-polarized optical traps can manipulate all structures described above. As an example, we demonstrate laser-controlled transportation of cholesteric CDs along the computer-programmed trajectories using time-shared dynamic laser traps [37], Fig. 2. These structures start to be attracted to the laser trap at distances less than  $3\mu m$

manipulation. For example, at powers  $30mW$  and larger, they allow one to produce dislocation kinks and anti-kinks [32] that mediate dislocation shift across the layers (along the microscope's optical axis), Fig. 3(h). Manipulation of the quadrupole of  $\lambda$ -disclinations, Fig. 4, also employs polarization dependence of the structure's effective refractive index, which can be varied from values smaller to higher than that of the LC around it. Both attractive and repulsive forces can be effectively used for optical manipulation. For example, the director structure in Fig. 4 is repelled from the linearly polarized laser trap with polarization perpendicular to it, but can be stretched and efficiently manipulated using two time-shared laser traps located at the opposite sides of the cluster.

### 3.3 Optical manipulation using high-intensity beams

Optical trapping with high-intensity focused laser beams is different from that described above. At high powers (usually  $\geq (30 - 45)mW$ , depending on the LC and cell thickness), a tightly-focused polarized laser beam [38, 39] locally reorients the director and produces elastic distortions, causing the optical Fredericksz transition [11, 12, 27, 29, 40-43]. This alters the optical trapping properties. For example, at powers  $< 40mW$ , the cluster shown in Figs. 4 and 5 is repelled from a focused beam with the linear polarization orthogonal to it. At higher powers, this beam locally reorients the director and exerts torsion on the structure, Fig. 5(a), 5(c), so that the disclinations in the cluster are locally parallel to the beam's polarization. The cluster with locally realigned director is then trapped by the beam and can be translated within the sample's plane. In a similar way, a cholesteric finger [Fig. 1(b)] can not be manipulated by a low-intensity beam with polarization perpendicular to the finger, as described above. However, the LC director is locally reoriented and trapping becomes possible at high powers; the focused laser beam causes local reorientation of the finger at powers  $> 100mW$ , similar to the case of the cluster shown in Fig. 5. Clearly, high-power laser beams allow the director structures to be not only spatially translated but even locally reoriented by changing the focused beam's polarization.

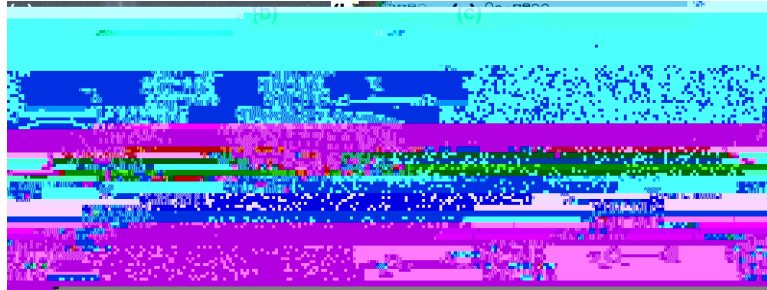


Fig. 5. (a). An image showing that a linearly-polarized beam of power  $W \approx 100mW$  exerts torsion and locally reorients an initially straight disclination cluster shown in Figs. 4. (b), 4(c) Schematics of the molecular alignment in the central part of (b) the undistorted cluster [similar to that shown in Fig. 4(h)] and (c) with the local laser-induced director reorientation that results in the structure trapping at high powers, as shown in (a). Crossed polarizers are along the image edges in (a).

## 4. Discussion

### 4.1 Refractive index contrast in liquid crystals with spatially-varying director

Polarized laser manipulation of the LC structures, Figs. 1-4, utilizes the spatially-



interface), the effective refractive index in LCs usually changes on the scale of microns. This is because the abrupt changes of LC director would be costly in terms of the elastic free energy [17, 18]. The exceptions are the structures containing defects with a singular core (such as point defects, line defects, and defect walls), at which the LC domains with strongly misaligned  $\hat{N}$  are joined, Fig. 1. These defects usually have the size of a core with undefined  $\hat{N}$  in the (10–100)*nm* range [17, 18]; from an optical standpoint, this corresponds to instant spatial changes of  $N$

$c$  is the speed of light,  $\omega$  is the size of the beam waist,  $W$  is the laser power,  $g$  is a coefficient of the order of unity that depends on the LC refractive indices, and  $\xi$  is the ratio between the focused beam size along  $\hat{z}$

$$\frac{2\xi(\omega^2 - 1)}{2\sqrt{2}\omega} \left[ \frac{\xi}{2\sqrt{2}\omega\xi} \right] \exp\left[-\frac{\xi^2}{8\omega^2}\right]$$

regime). Therefore, the laser trapping of director structures can be very complex and hard to describe analytically, especially in the LCs of strong optical anisotropy and at large depths of optical trapping.

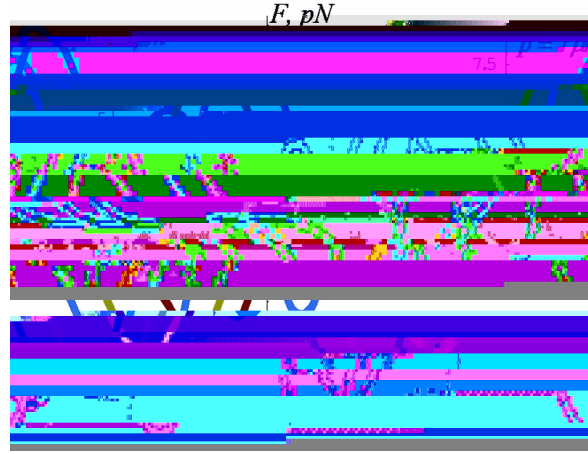


Fig. 7. Optical gradient forces calculated for the cholesteric CD and for power  $W = 15mW$ . The values of pitch  $p$  are marked for each curve. The trapping positions (zero force) are shown by the arrows. Note that large CDs can be trapped at a finite distance from their center.

#### 4.3 Optical manipulation assisted with the laser-induced director distortions

A laser beam of power exceeding the threshold  $W_h$  locally distorts the director  $\hat{N}$  [40-43] and changes the refractive index pattern, which then alters the optical gradient forces, Fig. 5. The maximum laser-induced change of local effective refractive index associated with the director realignment is  $\Delta n = n_e - n_o$ , which is sufficient to alter the optical trapping properties. The laser-modified pattern of an effective refractive index can be controlled by changing the polarization and power of the trapping beam, allowing one to further tune the optical trapping properties. In addition, laser trapping is modified by elastic structural forces between the structure and the laser-induced distortions, tending to minimize the elastic free energy

$$f_{elastic}(\vec{r}) = \frac{1}{2} \int [K_1 (\nabla \cdot \hat{N}(\vec{r}))^2 + K_2 (\hat{N}(\vec{r}) \cdot (\nabla \times \hat{N}(\vec{r})))^2 + K_3 (\hat{N}(\vec{r}) \times (\nabla \times \hat{N}(\vec{r})))^2] dV, \quad (7)$$

where  $\hat{N}(\vec{r})$  is the director field and  $\nabla$  is the gradient operator.

decreasing optical anisotropy and/or increasing the bend elastic constant  $K_3$  [40]. In planar cells (Figs.1(a), 3, 4, 5),  $W_{th}$  tends to be larger because of the LC's effect on the beam polarization [34, 41].  $W_{th}$  depends on the cell thickness  $h$  and the beam waist  $\omega$ , is larger for  $\omega/h \ll 1$  than for  $\omega/h \gg 1$  [41, 42], and can be within  $(10-300)mW$ , depending on the used trapping beams and LC cells. Finally, at very high powers (typically  $>500$